INTERNATIONAL JOURNAL FOR NUMERICAL METHODS IN FLUIDS, VOL. 8, 643–657 (1988)

ON VARIABLE GRIDS FOR MODELLING FLOW IN RECIPROCATING ENGINES

P. SHAH, N. C. MARKATOS

Centre for Numerical Modelling and Process Analysis, School of Mathematics, Statistics and Computing, Thames Polytechnic, London SE18 6PF, U.K.

AND

D. R. GLYNN

Concentration Heat and Momentum Ltd., Wimbledon, London SW19 5AU, U.K.

SUMMARY

The moving boundary (i.e. the piston) within a reciprocating engine poses the problem that as it moves towards the cylinder head it compresses the computational grid lines. Control cells that started with reasonable aspect ratios become so compressed that aspect ratios of 1000 are not unusual in some cases. This, of course, adversely affects numerical accuracy and convergence. It is the purpose of this paper to present a conservative scheme that allows for the removal and addition of grid cells, during simulation, so as to restore reasonable aspect ratios. Results of the computations are presented and compared with experimental data. It is concluded that with the proposed scheme convergence is obtained within fewer iterations, CPU time is reduced and the results are generally in better agreement with experimental data.

INTRODUCTION

The field of numerical modelling of Internal Combustion (IC) engines is developing rapidly and can be very useful for supplementing experimental knowledge of the flow field. Previous work[1–3] has identified several weaknesses even in the most sophisticated of the current models that handle three-dimensional transient problems. It is the purpose of this paper to highlight one of these weaknesses in particular, namely the ill-conditioned cells arising when the grid above the piston is compressed, and to propose a solution to the problem.

THE PHYSICAL PROBLEM

The simulation is concerned with the flow of air in the combustion chamber of a diesel engine during compression and expansion. Motoring conditions are considered for simplicity.

0271-2091/88/060643-15$07.50

Received 16 October 1986
Revised 29 June 1987

The geometry considered is similar to the Ricardo direct-injection E16 single-cylinder, four-stroke diesel engine and is illustrated in Figure 1. The engine specifications are as follows:

Bore	120.65	mm
Stroke	139.7	mm
Piston/head clearance	1.08	mm
Compression ratio	16:1	
Engine speed	24	revs/s
IVC	41°	ABDC
EVO	110°	ATDC.

The flow is predicted at a series of times between inlet valve closure (IVC), which occurs at 41° ABDC, and exhaust valve opening (EVO), which occurs at 110° ATDC.

The calculations described in this paper are two-dimensional and assume that the flow is rotationally symmetrical. Details on the actual asymmetry of the engine studied and comparisons between 2D and 3D predictions for the same engine are given in Reference 4.

THE MATHEMATICAL MODEL

The model consists of the set of time-dependent, partial-differential, source balance equations that express the conservation of mass, momentum, energy and other conserved fluid variables in recirculating transient flows. The k–ε model of turbulence has been used.[4]

The finite-domain equations are obtained by integrating the partial differential equations over control volumes.

The finite-difference grid consists of a fixed part within the piston bowl and an expanding contracting part above the piston crown which varies with the motion of the piston. The irregular geometry of the piston shape (i.e. bowl) has been accommodated by the use of 'cell porosities'.[4] While body-fitted co-ordinates provide a better approach, the present one is adequate for this

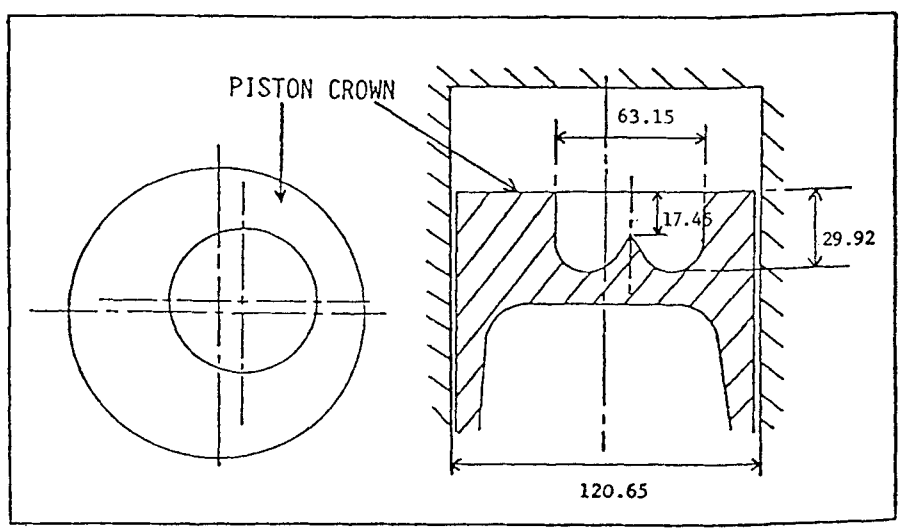

Figure 1. Piston-in-cylinder geometry (dimensions in mm)

study, where the numerical procedure is of principal interest. The solution algorithm is the 'SIMPLEST' algorithm of Spalding.[5]

THE PROBLEM OF COMPRESSED GRIDS

General

The grid distances above the piston crown vary during the solution procedure, as the piston compresses the grid lines towards top dead centre (TDC) and expands them past TDC. This is illustrated schematically in Figure 2, which shows clearly how the cells above the piston become elongated as TDC is approached.

In order to obtain a reasonably accurate representation of the flow in the earlier stages of the cycle, the space between the cylinder head and the piston must be divided into a considerable number of cells. As TDC is approached, however, this will mean that the cells in this region become very long and thin. In a typical calculation the aspect ratios vary from 1·3 at IVC to 131·7 at TDC; the latter value may not be acceptable for a numerical calculation.

A simple conservative scheme has been devised to overcome the above problem. Grid cells in the axial direction are progressively removed (before TDC) or added (after TDC) to reduce excessive aspect ratios. It is of course necessary to ensure that, when grid cells are added or removed, the total mass and momentum in the system are unaffected. The technique described below is designed to achieve this in the simplest possible way. More general (and complicated) schemes may be found in References 6 and 7.

For simplicity, the description that follows refers to a uniform grid above the piston. Generalization to non-uniform 3D grids is straightforward.

Removal of grid cells

Consider the uniform mesh of Figure 3(a). The velocities are stored at the cell faces and scalar variables are stored at the cell centres. The situation is originally as shown in Figure 3(a) and it is to be adapted to that shown in Figure 3(b).

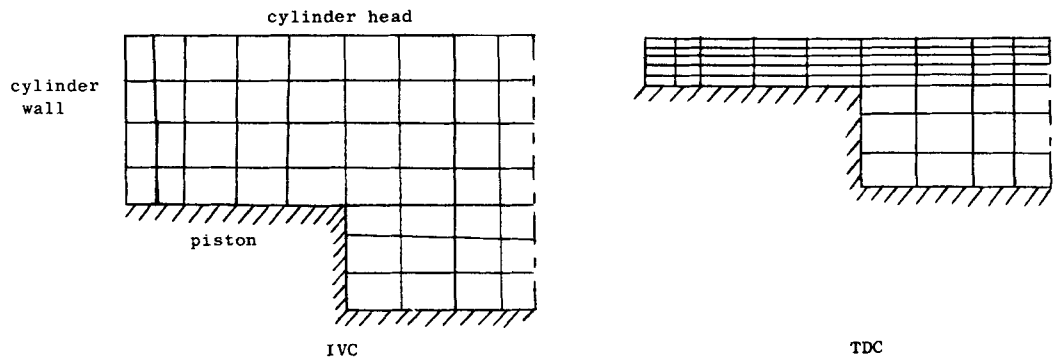

Figure 2. Schematic representation of grid at IVC and TDC

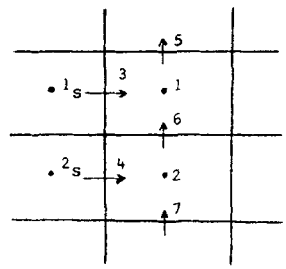

Figure 3(a)

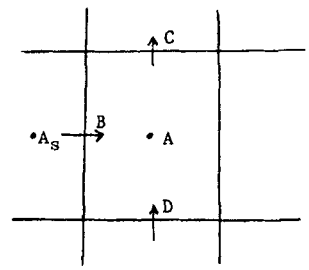

Figure 3(b)

The values of the variables for the mesh in Figure 3(b) are obtained from those for the mesh in Figure 3(a) by applying the conservation laws as follows:

mass conservation

$$\rho_A=(\rho_1+\rho_2)/2,$$

ϕ-conservation

$$\rho_A\phi_A=(\rho_1\phi_1+\rho_2\phi_2)/2, \quad \text{where } \phi=k,\varepsilon,u,$$

pressure

$$p_A=(p_1+p_2)/2,$$

axial velocity

$$W_C=W_5, \qquad W_D=W_7,$$

mass conservation at lateral face

$$V_B\rho_{B,up}=(V_3\rho_{3,up}+V_4\rho_{4,up})/2,$$

where the subscript 'up' refers to the upwind density at the appropriate locations, given by

$$\rho_{3,up}=\begin{cases}\rho_{1s} & \text{for } V_3\geqslant 0,\\ \rho_1 & \text{for } V_3<0\end{cases}$$

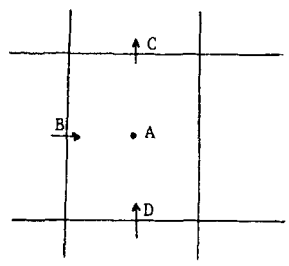

Figure 4(a)

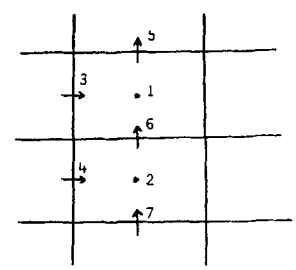

Figure 4(b)

and similarly for $\rho_{4,up}$.

Also

$$\rho_{B,up}=\begin{cases}\rho_{A_s} & \text{for} \quad V_3\rho_{3,up}+V_4\rho_{4,up}\geq 0,\\ \rho_A & \text{for} \quad V_3\rho_{3,up}+V_4\rho_{4,up}<0.\end{cases}$$

Addition of grid cells

After TDC, as the piston descends, extra grid cells must be added. Thus it is required to subdivide the cell in Figure 4(a), as shown in Figure 4(b), and the values for the variables identified on the new mesh are required as follows:

$$\rho_1=\rho_2=\rho_A,$$

$$\phi_1=\phi_2=\phi_A, \quad \text{where } \phi=p,k,\varepsilon,u,$$

$$W_5=W_C, \qquad W_6=(W_C+W_D)/2, \qquad W_7=W_D,$$

$$V_3=V_4=V_B.$$

General considerations

The above procedure is carried out at a given set of crank positions, selected in advance, but it is easy to arrange for the program to decide automatically, based on the criterion of aspect ratios not exceeding, say, 20.

Coding this procedure involves careful consideration of the order in which the values of the

Table I. Grid sizes considered

Case number	Grid size $Y\times Z$	Number of grid cells above piston crown	Number of grid cells in bowl
1	11×15	8	7
2	19×28	16	12
3	28×40	16	24
4	40×60	24	36

Table II. Example of variation in number of cells

Crank position (degrees after TDC)	Total number of grid cells in axial direction	Number of grid cells above piston crown
−94	15	8
−47	11	4
−18	9	2
0	8	1
18	8	1
72	9	2
110	11	4

variables for the 'old' grid are replaced by the 'new' values; this is important in saving space and time during computations.

Computational details

Four different grid sizes (cases 1–4) were employed with totals of 130 and 260 time-steps to cover a crank advance of 250°. The situation at IVC is as shown in Table I.

All four cases were run with the adaptive grid technique. The first two cases were also run with non-adaptive grids. To illustrate the adaptation of the grid during the solution procedure, consider the 11 × 15 grid. The 15 cells in the axial direction initially comprise seven in the piston bowl and eight above the piston. The number above the piston changes during the course of the computation, as shown in Table II.

Many runs were performed to obtain the optimum grid size, time-step and number of iterations per time-step. These will be described in the next section.

RESULTS AND DISCUSSION

Grid-independency studies

Figures 6–9 show swirl and axial velocity profiles at a radial distance of 18.9 mm (Figure 5) away from the bowl centre. The profiles are at 47° before top dead centre (BTDC) and 27° BTDC for Figures 6, 8 and Figures 7, 9 respectively for the four different grid sizes considered.

It is clear that the results tend towards grid independency and that for the purpose of the current work a 19 × 28 grid is quite adequate.

Time-step-independency studies

Two runs using 130 and 260 time-steps were selected to cover a crank advance of 250°. From the results it is clear that using 130 time-steps is adequate.

Mass and angular momentum

Figure 10 shows the total mass in the system at the end of every ten time-steps for case 2 when the adaptive grid technique is used. It is clear that this remains constant, as expected. Also the corresponding total angular momentum (Figure 11) shows the correct physical trend, i.e. a steady fall due to the influence of wall friction.

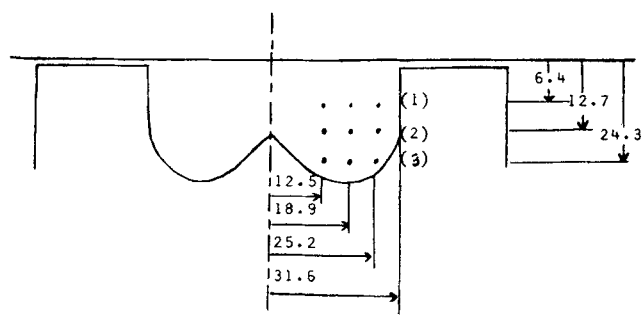

Figure 5. Measurement positions (dimensions in mm)

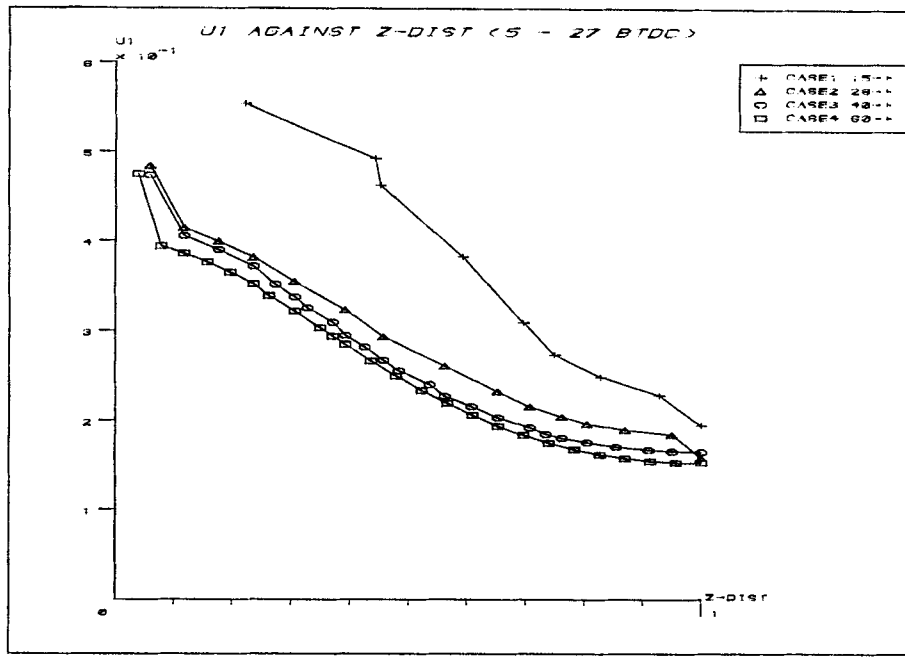

Figure 6. Swirl velocity profiles at 47° BTDC

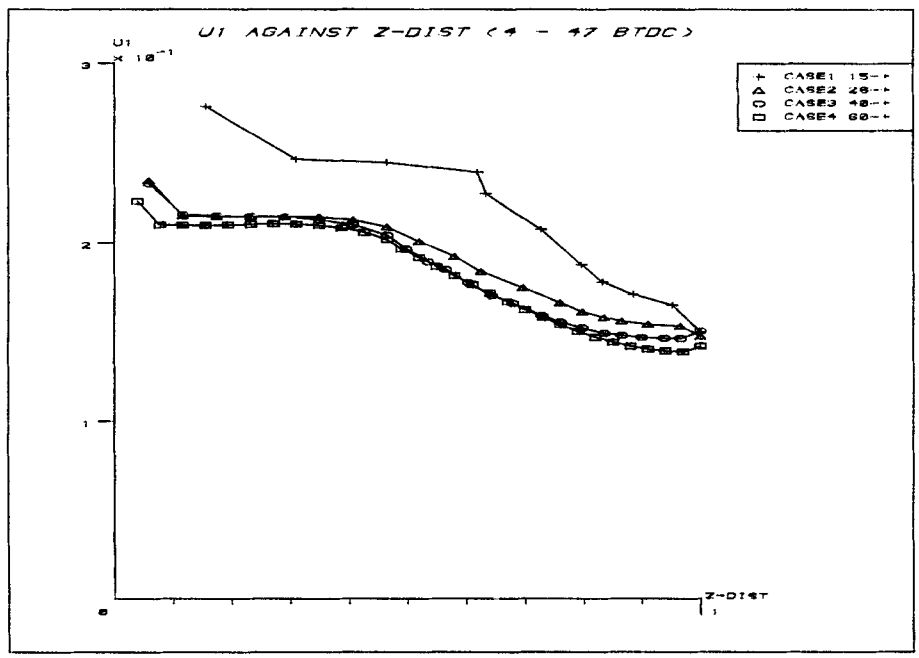

Figure 7. Swirl velocity profiles at 27° BTDC

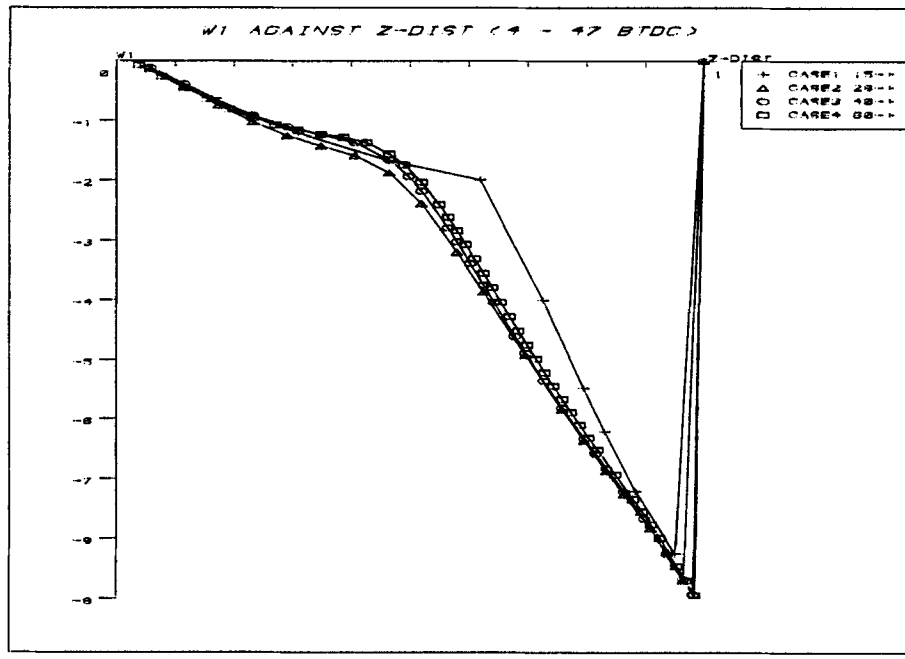

Figure 8. Axial velocity profiles at 47° BTDC

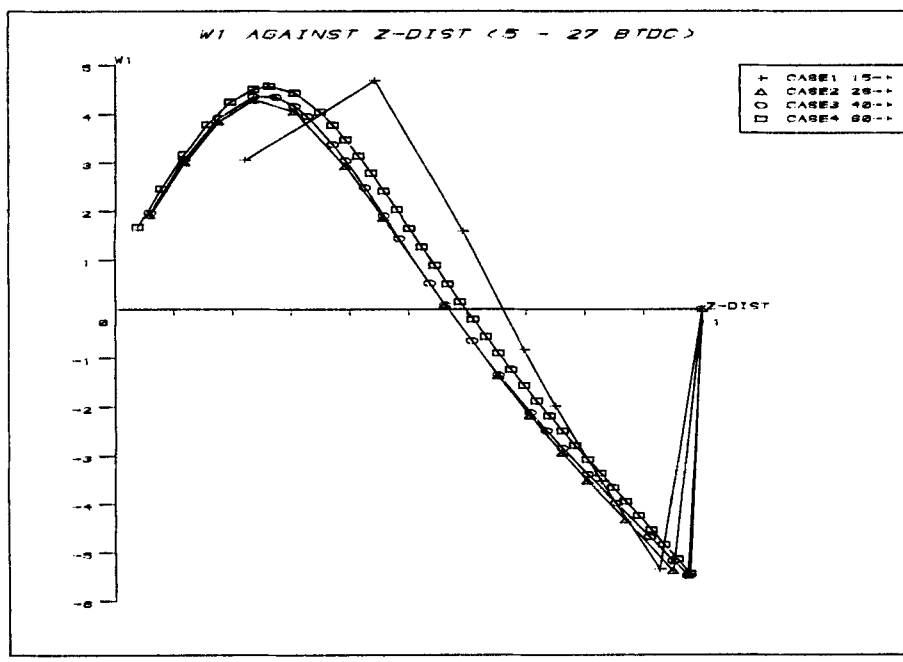

Figure 9. Axial velocity profiles at 27° BTDC

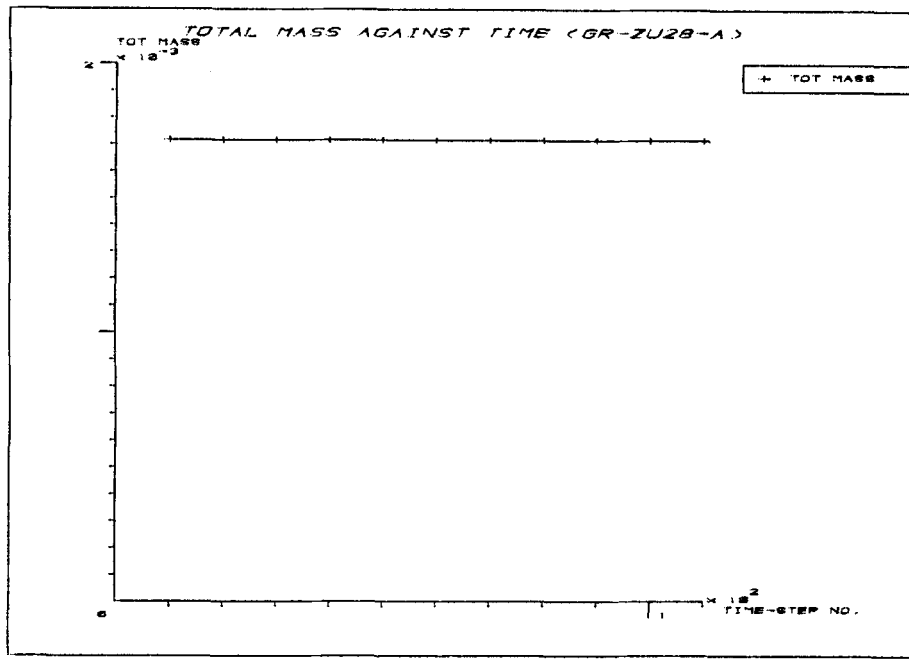

Figure 10. Plot of total mass in the system against time

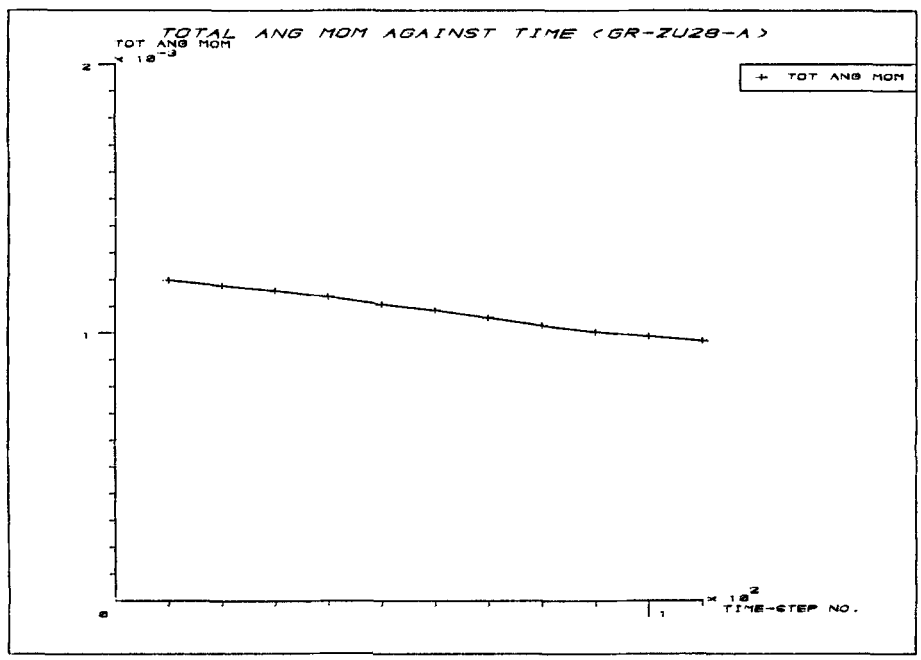

Figure 11. Plot of total angular momentum in the system against time

Computer time requirements

Figure 12 shows the CPU time per ten time-steps required for the same convergence criterion with and without the adaptive grid technique for case 1. It is clear that CPU time requirements decrease considerably (by about 60% at TDC) when the adaptive grid technique is utilized.

Convergence

The CPU time savings were obtained partly because of the smaller number of grid cells near TDC but also because near TDC, where convergence is most difficult, fewer iterations (typically 40 iterations compared with 80 without the adaptive grid technique) were required. It was also found that as the grid was refined further than 28×40 it was extremely difficult for the solution to converge at all when the adaptive grid technique was not utilized, because of the extreme aspect ratios involved.

Comparison with experiment

Results for comparison with experiment are presented at the locations in the piston bowl shown in Figure 5. These positions correspond to Ricardo's experimental results.

It should of course be borne in mind that the calculations have been made with the assumption of axisymmetry; the offset of the bowl will lead to some discrepancy in the predictions.[4]

The results presented below are for case 2. Swirl velocity is plotted at depths (1), (2) and (3): 6·4, 12·7 and 24·32 mm below the piston crown respectively.

Swirl velocity profiles (Figures 13–15) are given for seven crank positions: 27° BTDC, 18° BTDC, 9° BTDC and TDC, 9° ATDC, 18° ATDC and 27° ATDC, labelled 1, 2, 3, 4, 5, 6 and 7 respectively on the figures. RMS turbulence velocity profiles presented in Figures 16–18 are at TDC and the labels 1, 2 and 3 on the figures represent the three bowl depth positions respectively.

It is clear from these plots and Table III that the adaptive grid technique improves agreement with experiment. Table III shows the average percentage error at TDC (for cases 1 and 2) without and with grid adaptation. The average percentage errors for swirl velocity and turbulence velocity are obtained at 24·32 and 6·4 mm below the piston crown respectively.

For case 2 the adaptive grid technique improves agreement with swirl velocity to approximately 27% and overpredicts turbulence velocity up to approximately 131%, as compared with 59% and 152% respectively without the adaptive grid technique.

CLOSURE

A simple technique has been devised to allow for removal or addition of grid cells as the crank angle advances, so as to restore reasonable cell aspect ratios. Although this technique is not of course unique, and indeed others have already been devised,[6,7] it is still a simple and reliable technique that is also consistent with the order of accuracy of the finite difference scheme used. The great advantage of this procedure is that convergence is significantly improved, particularly for fine grids. Fewer iterations per time step are required and good convergence is achieved even in cases where it is difficult if the technique is not used. Furthermore, accuracy is also seen to improve, the technique is simple to implement and is applicable to any fluid flow problem with an expanding or contracting grid.

Experimental data for the cases under consideration are limited, but comparison between the predictions and measurements shows better agreement when the new technique is employed.

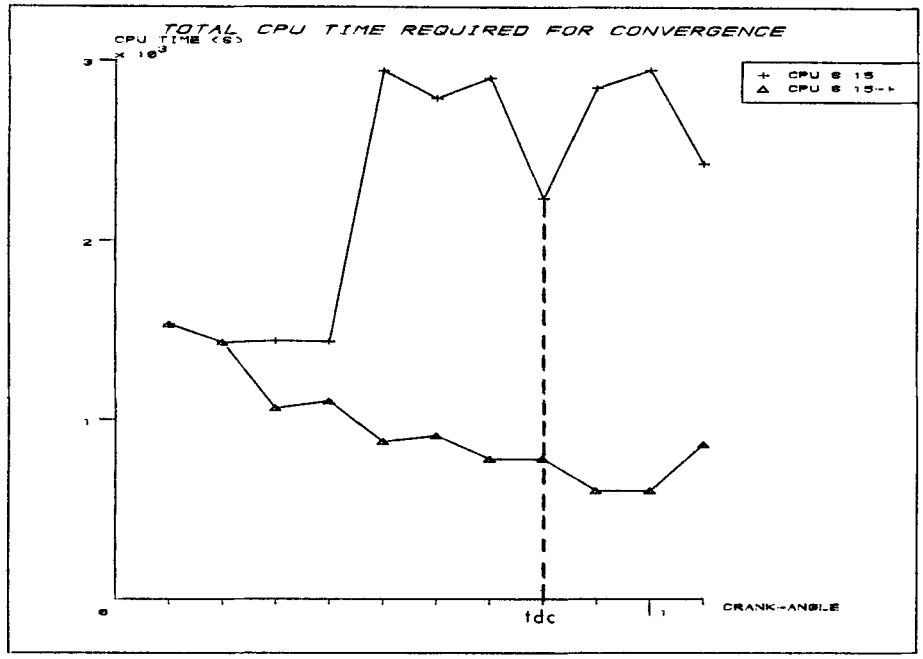

Figure 12. Total CPU time required for convergence with and without grid adaption

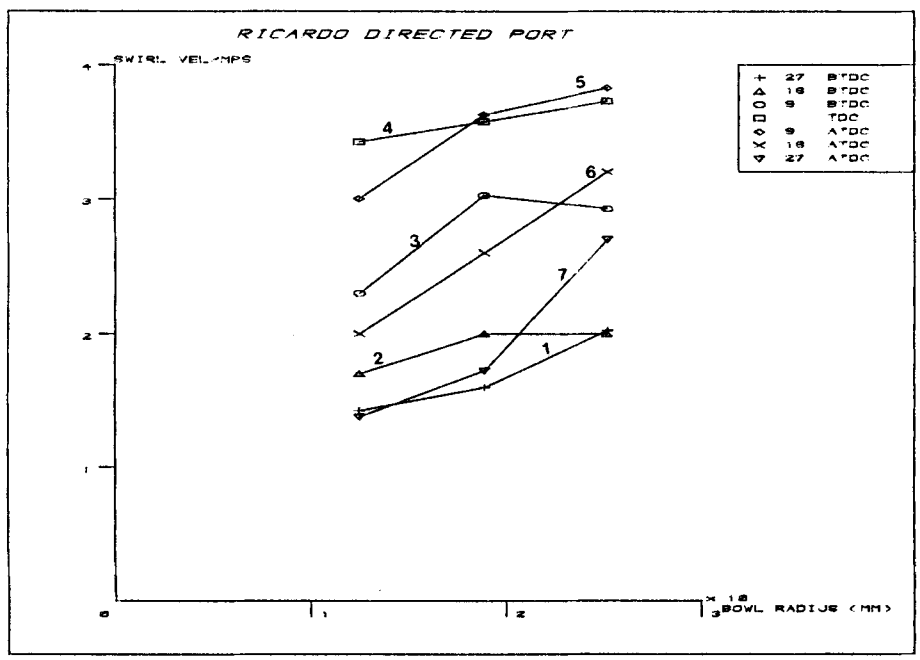

Figure 13. Swirl velocity Ricardo measurements

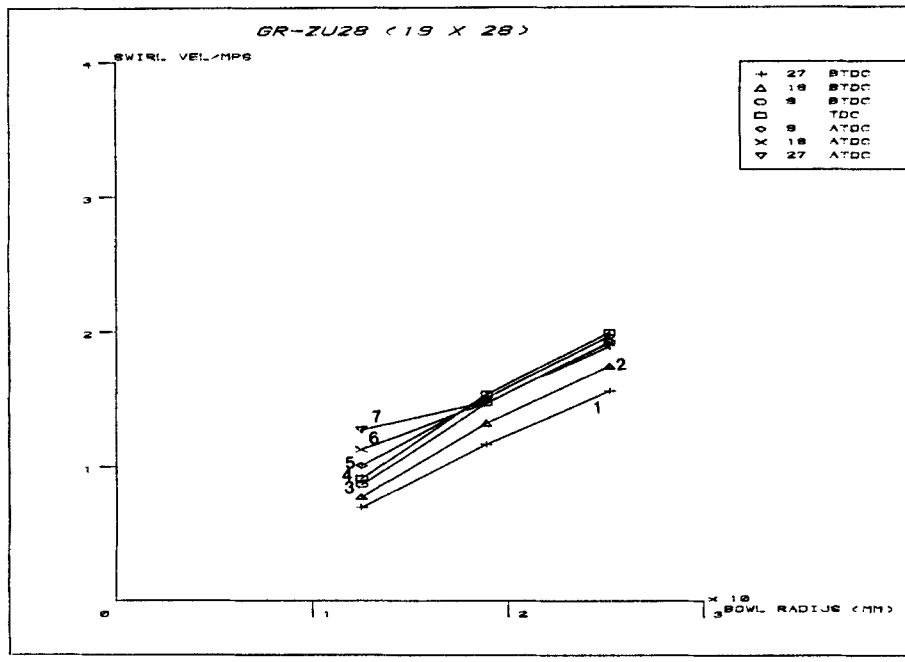

Figure 14. Swirl velocity without grid adaption

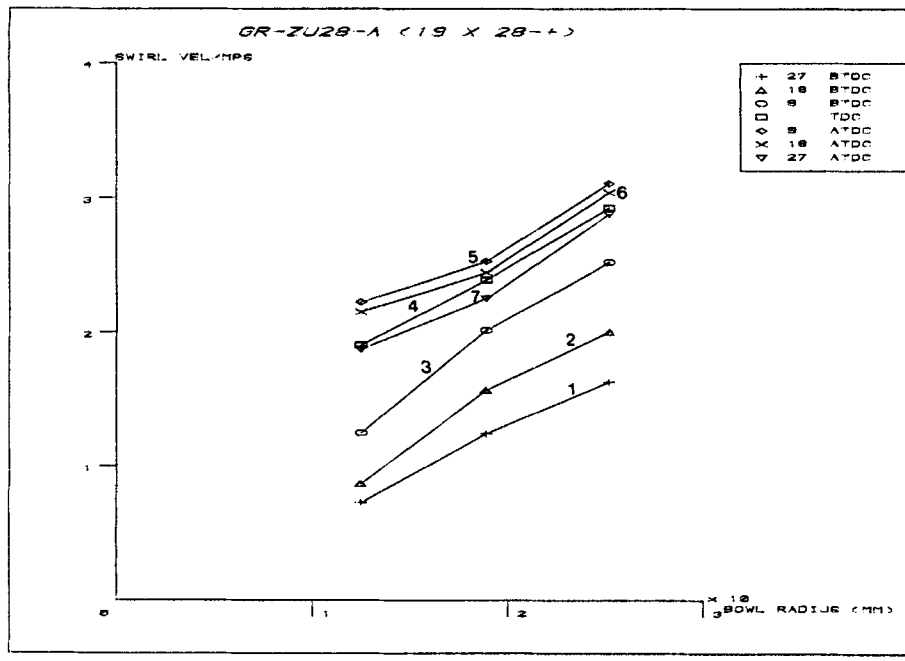

Figure 15. Swirl velocity with grid adaption

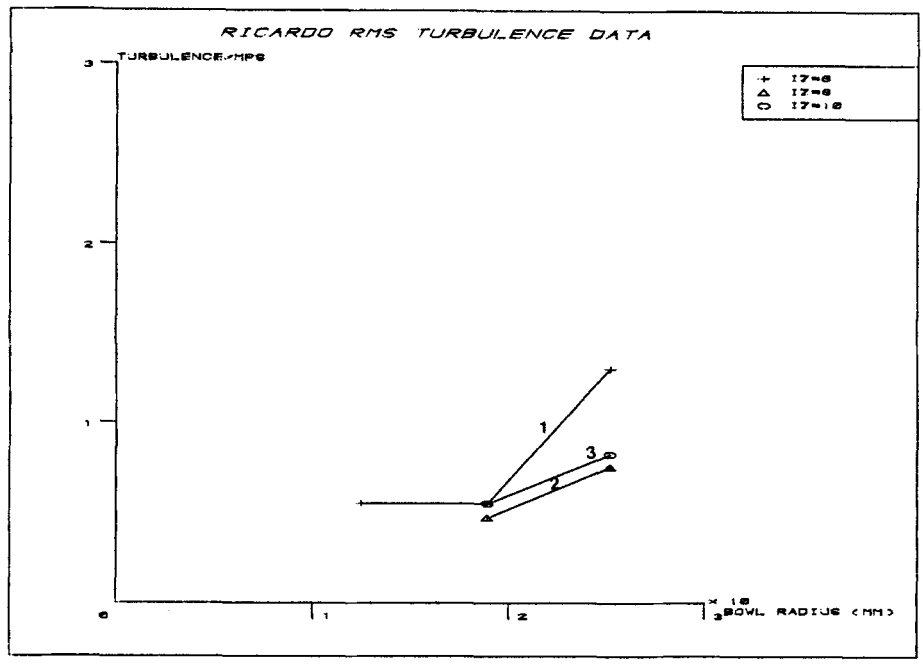

Figure 16. RMS turbulence Ricardo measurements

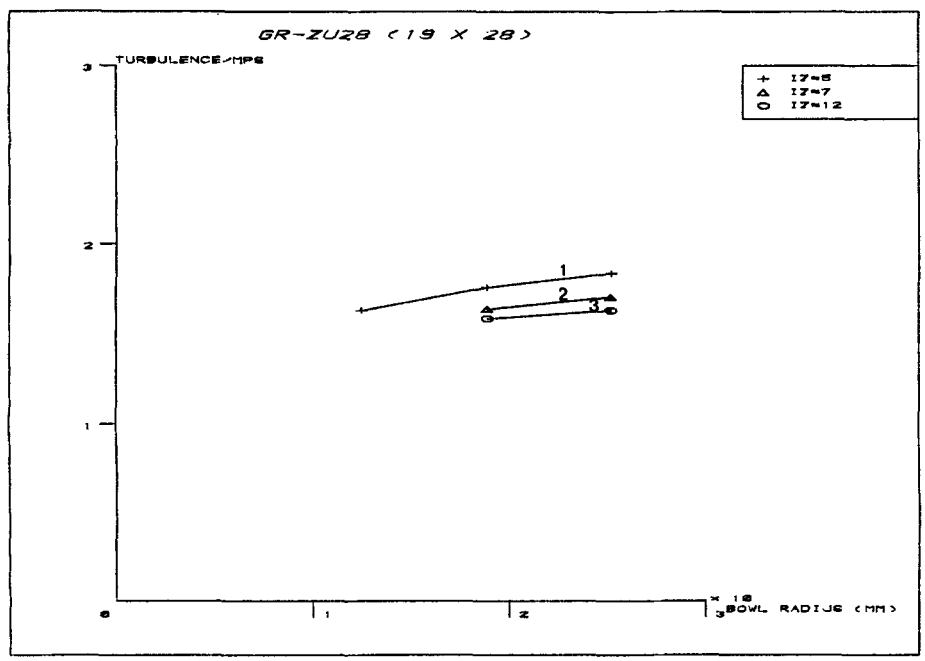

Figure 17. RMS turbulence without grid adaption

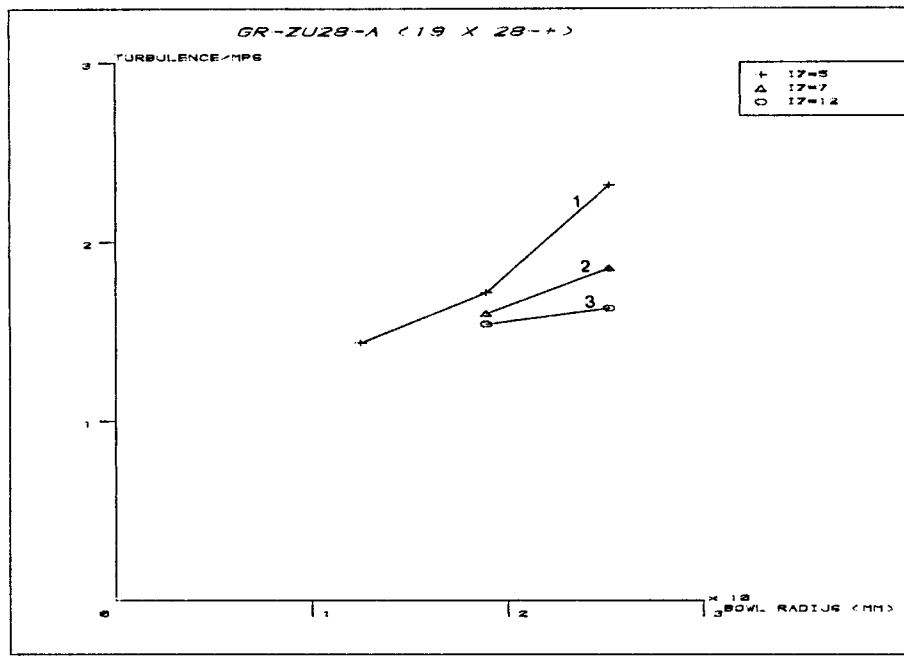

Figure 18. RMS turbulence with grid adaption

Table III. Average percentage error

Case number*	Average percentage error		
	Grid size	Swirl velocity	Turbulence velocity
1	11 × 15	18·17	62·2
1(− +)	11 × 15	11·28	46·2
2	19 × 28	59·00	152·4
2(− +)	19 × 28	27·3	131·6

* (− +) = grid adaptation included.

ACKNOWLEDGEMENTS

The authors wish to thank Dr. D. G. Tatchell of CHAM Ltd. and Dr. C. W. Richards of Thames Polytechnic for their advice on this work. Permission by CHAM Ltd. to use their general program PHOENICS is gratefully acknowledged.

REFERENCES

1. S. F. Benjamin, J. H. Weaving, D. R. Glynn, N. C. Markatos and D. B. Spalding, 'Development of a mathematical model of flow, heat transfer and combustion in a stratified-charge engine', *Inst. Mech. Eng. Stratified Charge Automotive Engine Conf., Paper C403/89*, November 1980, pp. 91–99.
2. N. C. Markatos and T. Mukerjee, '3D computer analyses of flow and combustion in atutomotive internal combustion engines', *Math. Comput. Simul.*, **XXIII**, 354–366 (1981).
3. P. Shah and N. C. Markatos, 'Turbulence modelling in internal combustion engines', *Proc. Fourth Int. Conf. on Numerical Methods in Laminar and Turbulent Flow*, Part 2, Pineridge Press, Swansea, 1985, pp. 1439–1454.
4. P. Shah and N. C. Markatos, 'On the 2D and 3D computer analyses of turbulence in internal combustion engines', *ASME Paper No. 87-FE-12*, 1987, pp. 1–10.
5. D. B. Spalding and N. C. Markatos, 'The mathematical basis of Phoenics', *Phoenics Lecture Notes 3*, 1982.
6. Man Mohan Rai, 'A conservative treatment of zonal boundaries for Euler equation calculations', *J. Comput. Phys.* **62,** 472–503 (1986).
7. M. Berger and J. Oliger, 'Adaptive mesh refinement for hyperbolic partial differential equations', *J. Comput. Phys.* **53,** 484–512 (1984).